

## Phase Noise Effect on Frequency Measurement Error of IFM Receivers

Ken'ichi TAJIMA, Kenji KAWAKAMI, Akiho KAGOHARA and Kenji ITOH

Information Technology R&D Center, Mitsubishi Electric Corp.

5-1-1 Ofuna, Kamakura-city, Kanagawa 247-0056, JAPAN

TEL: 0467-41-2549, FAX : 0467-41-2519, E-mail : ktajima@micro4.isl.melco.co.jp

### ABSTRACT

This paper presents phase noise effect on frequency measurement errors of an IFM (Instantaneous Frequency Measurement) receiver. In the paper, a calculation method of frequency measurement errors due to phase noise of a PLL synthesizer for an local oscillator is discussed. Calculated results indicate, (1) Phase noise effect on frequency measurement error is clarified, (2) Frequency measurement errors can be reduced by narrowing a noise bandwidth of the PLL synthesizer when integrated phase noise in the noise bandwidth remains constant. Moreover, calculated results are verified by measured results with a developed 5 to 10 GHz PLL synthesizer.

### I. INTRODUCTION

In this paper, phase noise effect on frequency measurement errors of an IFM (Instantaneous Frequency Measurement) receiver[1] is discussed. An IFM receiver determines frequency of incoming signal after an RF signal is down-converted to IF band. Thus, a wide-band frequency synthesizer[2], used for an local oscillator of a frequency converter, is required for a wide-band reception. An analog direct synthesizer is generally employed, since this synthesizer has following characteristics: (a) low phase noise and low spurious level, (b) wide-band and narrow channel steps, and (c) fast frequency switching speed[2]. However, size of this synthesizer is large, because it consists of many components like phase locked oscillators, mixers and filters. On the other hand, a PLL synthesizer[2] with a single loop topology is small in size. Yet, a PLL synthesizer with this topology does not have superior phase noise characteristics compared to an analog direct synthesizers since the PLL synthesizer consists of low Q VCO for wide-band oscillation[3].

When phase noise of the PLL synthesizer, thermal noise given by the IFM receiver's noise figure, and spurious emissions of the frequency converter are added to an incoming signal of the IFM receiver, frequency measurement errors of the IFM receiver[4] are caused. In the past, there were reports that discussed thermal noise effect on frequency measurement errors of an IFM receiver[4],[5]. However there is no report about phase noise effect on frequency measurement errors.

This paper presents phase noise effect on frequency measurement errors of the IFM receiver by a simulation method. In this simulation method, an inputted signal is defined with phase noise, thermal noise and spurious emissions. Then the inputted signal is processed according to a configuration of the IFM receiver. Finally, a parameter which represents frequency measurement errors is calculated to clarify phase noise effect. Moreover, measured results with a developed 5 to 10 GHz PLL synthesizer indicate adequacy of the simulation program.

### II. FREQUENCY MEASUREMENT ERRORS OF THE IFM RECEIVER

#### A. CONFIGURATION

A configuration of the IFM receiver is shown in Fig.1. The IFM receiver consists of an RF front-end section and IFM detection section. The RF front-end section consists of LNA, BPF1, Mixer and PLL synthesizer (frequency:  $f_o$ ), and down-converts an incoming RF signal (frequency:  $f_{in}$ ) to IF signal (frequency:  $f_{if}$ ). The IFM detection section consists of BPF2, amplifier, quadrature detector and two LPFs (LPF<sub>i</sub> and LPF<sub>q</sub>), and outputs voltages ( $V_i$  and  $V_q$ ) which give frequency of the incoming signal. At this quadrature detector, the IF signal is divided into two signals in phase by an in-phase divider1. An output signal from the in-phase divider1 is inputted to a delay line with delay time  $\tau$ . Another output signal from the in-phase divider1 is inputted to a 90° hybrid circuit. An output signal from the delay line is inputted to an in-phase divider2. Then output signals from the in-phase divider2 are inputted to mixers (Mixer<sub>i</sub> and Mixer<sub>q</sub>). Also, output signals from the 90° hybrid circuit are inputted to mixers. Inputted signals are multiplied at mixers, and results are outputted to LPFs. LPFs output voltages by reducing bandwidth of the outputted signals from mixers.

The IFM receiver measures frequency of the incoming signal by a differential detection. This measured frequency  $f_{in}$  is determined by output voltages ( $V_i$  and  $V_q$ ) and delay time  $\tau$  of the delay line, is given as follows:

$$f_{in} = f_o + \theta / (2\pi \cdot \tau), \theta = \tan^{-1}(V_i / V_q) \quad (1)$$

According to (1),  $\theta$  is varied from  $-\pi$  to  $\pi$ , thus measurable frequency range of  $f_{in}$  is  $f_o - 0.5\tau$  to  $f_o + 0.5\tau$ .

#### B. FREQUENCY MEASUREMENT ERRORS

Phase noise and thermal noise effect on measurement frequency errors are discussed. A distribution of output voltages ( $V_i$  and  $V_q$ ) is shown in Fig.2(a). In this case, neither phase noise and thermal noise is added to the incoming signal. There is no dispersion of angular phase  $\theta$  as shown in Fig.2(a). Another distribution of output voltages ( $V_i$  and  $V_q$ ) is shown in Fig.2(b). In this case, only thermal noise is added to the incoming signal. There is dispersion of angular phase  $\theta$  as shown in Fig.2(b), since thermal noise is added to each amplitude of output voltages ( $V_i$  and  $V_q$ ). Thermal noise does not correlate with the incoming signal, thus a dispersion of  $\theta$  becomes larger as added thermal noise becomes larger. A distribution of output voltages ( $V_i$  and  $V_q$ ) is shown in Fig.2(c). In this case, only phase noise is added to the incoming signal. There is dispersion of angular phase  $\theta$  as shown in Fig.2(c). Frequency measurement errors are caused by the dispersion of  $\theta$  as shown in Fig.2(b) and 2(c). This paper discusses frequency measurement errors due to the dispersion of  $\theta$  by a simulation method.

### III. SIMULATION PROGRAM

#### A. FLOW CHART OF SIMULATION PROGRAM

A flow chart of a simulation program is shown in Fig.3. This simulation program calculates frequency measurement errors according to a configuration shown in Fig.1. Furthermore, the simulation program uses FFT for transforming data in time domain to frequency domain and vice versa.

Descriptions of each calculation step of the simulation program as shown in Fig.3(a) are discussed. For step 1, parameters for the simulation program are inputted. Inputted parameters are, (1) Level of the incoming signal, (2) Level of thermal noise, (3) Offset frequency and level of spurious emissions, and (4) delay time of delay line. For step 2, the incoming signal is defined with phase noise in frequency domain as shown in Fig.3(b). For step 3, the incoming signal is defined with spurious emissions in frequency domain as shown in Fig.3(c). For step 4, the incoming signal is defined with thermal noise in frequency domain as shown in Fig.3(d). The value of added thermal noise includes noise figure of the IFM receiver. For step 5, a bandwidth of the incoming signal is reduced by a BPF2 in frequency domain. For step 6, the incoming signal is inputted to a quadrature detector, and is outputted as two voltages.

Descriptions of step 6 in more details are discussed. For step 6a, the inputted IF signal is divided into two signals  $A(f)$  and  $B(f)$  by the in-phase divider1 in frequency domain. For step 6b, the signal  $A(f)$  is delayed by  $\tau$  at the delay line in frequency domain. A delayed signal  $A\tau(f)$  is given as follows:

$$A\tau(f) = A(f) \cdot e^{2\pi f\tau} \quad (2)$$

For step 6c, the signal  $A\tau(f)$  is divided into two signals  $A_i(f)$  and  $A_q(f)$  by an in-phase divider2 in frequency domain. These two outputted signals  $A_i(f)$  and  $A_q(f)$  are inputted into Mixer<sub>i</sub> and Mixer<sub>q</sub> respectively. For step 6d, the signal  $B(f)$  is divided into two signals  $B_i(f)$  and  $B_q(f)$  by the 90° hybrid circuit in frequency domain. The signal  $B_q(f)$  is off 90° from the signal  $B(f)$ , and is given as follows:

$$B_q(f) = B(f) \cdot e^{\pi/2} \quad (3)$$

These two outputted signals  $B_i(f)$  and  $B_q(f)$  are inputted into Mixer<sub>i</sub> and Mixer<sub>q</sub> respectively. For step 6e, two inputted signals of Mixer<sub>i</sub> and Mixer<sub>q</sub> are multiplied in time domain. These Mixer<sub>i</sub> and Mixer<sub>q</sub> are considered as linear multipliers. Thus, output signals of mixers  $C_i(t)$  and  $C_q(t)$  are given as follows:

$$C_i(t) = A_i(t) \cdot B_i(t), \quad C_q(t) = A_q(t) \cdot B_q(t) \quad (4)$$

These two outputted signals  $C_i(t)$  and  $C_q(t)$  are inputted into LPF<sub>i</sub> and LPF<sub>q</sub> respectively. For step 7, a bandwidth of outputted signals  $C_i(t)$  and  $C_q(t)$  are reduced by LPF<sub>i</sub> and LPF<sub>q</sub> in frequency domain. Then voltages  $V_i$  and  $V_q$  are outputted from LPF<sub>i</sub> and LPF<sub>q</sub>. For step 8, according to (1), measured frequency  $f_{inj}$  is calculated from outputted voltages  $V_i$  and  $V_q$ . Then frequency deviation  $\sigma$  is calculated, and is given as follows:

$$\sigma = \sqrt{\frac{1}{q} \sum_{j=1}^q (f_{inj} - f_{mean})^2}, \quad f_{mean} = \frac{1}{q} \sum_{j=1}^q f_{inj} \quad (5)$$

where  $q$  is number of calculated data and  $f_{inj}$  ( $j=1, \dots, q$ ) is calculated results of  $f_{inj}$ .

#### B. GENERAL PROPERTIES WITH PHASE NOISE EFFECT

Calculated results of a distribution of  $V_i$  and  $V_q$  with addition of thermal noise  $C/N=25$  dB is shown in Fig.4. Calculated results in Fig.4 has similar distribution of output voltages shown in Fig.2(b). Calculated results of a distribution of  $V_i$  and  $V_q$  with addition of phase noise as shown in Fig.5(b), is shown in Fig.5(a). Calculated results in Fig.5(a) has similar distribution of output voltages shown in Fig.2(c).

Calculated results of frequency deviation  $\sigma$  versus offset frequency is shown in Fig.6. In this figure,  $\sigma$  is normalized by  $180/(\pi\tau)$ , and offset frequency is normalized by  $1/\tau$ . From Fig.6, frequency measurement errors will not be caused at offset frequency equals to harmonics of frequency  $1/\tau$ . Since  $\sigma$  becomes 0 with period of  $1/\tau$ . This is characteristic of a differential detection.

Calculated results of frequency deviation  $\sigma$  with constant integrated phase noise in the noise bandwidth of the PLL synthesizer is shown in Fig.7. In this figure, the noise bandwidth is normalized by  $1/\tau$ , and  $\sigma$  is normalized by  $180/(\pi\tau)$ . A model of phase noise used for the simulation is shown in Fig.7(a). From Fig.7(b),  $\sigma$  has the maximum value at  $1/\tau=1.25$ . Also, frequency measurement errors can be reduced by narrowing a noise bandwidth of the PLL synthesizer when integrated phase noise in the noise bandwidth remains constant.

#### IV. MEASURED RESULTS

Parameter summary for measurement and calculation is shown in table 1. A configuration as shown in Fig.1 is used for measurement and calculation. A harmonic mixer is employed for a mixer in RF front-end section. Thus phase noise and spurious emissions of the PLL synthesizer are doubled by a harmonic mixer. Measured and calculated results of frequency deviation  $\sigma$  with  $\tau = 800$  ns is shown in Fig.10. Integrated phase noise is -33 dBc/100 kHz approximately. From Fig.10, calculated results has a good agreements with a measured results. Also, there is a measurement limit ( $\sigma=35$  kHz with  $C/N>30$  dB) due to addition of phase noise. There is small effect by spurious emissions to a degradation of  $\sigma$ , since spurious level of -46 dBc is negligibly small compared with phase noise shown in Fig.5(b).

#### V. CONCLUSION

This paper presents phase noise effect on frequency measurement errors of the IFM receiver. In the paper, a calculation method to determine frequency measurement errors due to phase noise is discussed. Calculated results by the simulation indicate, (1) Frequency measurement error due to phase noise is clarified, (2) Frequency measurement errors can be reduced by narrowing a noise bandwidth of the PLL synthesizer when integrated phase noise in the noise bandwidth remains constant. Moreover, measured results with a developed 5 to 10 GHz PLL synthesizer indicates adequacy of calculated results.

## REFERENCE

- [1] J.B. TSUI, "Digital microwave receivers - theory and concepts," Artech House, 1989.
- [2] V. MANASSEWITSCH, "Frequency synthesizer theory and designs," 3rd edi., John Wiley & Sons, 1986.
- [3] V.F. KROUPA, "Noise properties of PLL systems," IEEE Trans. Comm. vol. COM-30, no.10, pp2254-2253, 1982.
- [4] "Performance of DFD's in the presence of noise," Anaren Microwave publication M1820-08.
- [5] P.W. East, "Design techniques and performance of digital IFM," IEEE Proc., vol. 129, no.3, June 1982.
- [6] K. Tajima, Y. Imai, Y. Kanagawa, K. Itoh, Y. Isota, O. Ishida, "A 5 to 10 GHz low spurious triple tuned type PLL synthesizer driven by a DDS for an IFM receiver," 1997 IEEE MTT-S International Microwave Symposium Digest, pp.1217-1220, June 1997.

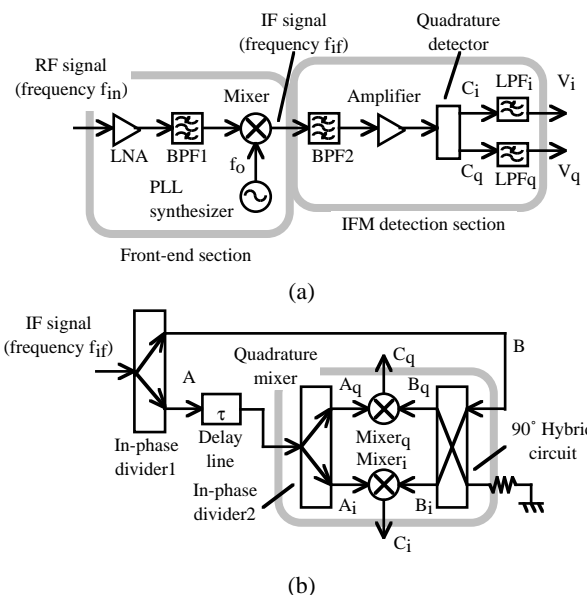


Fig.1. Configuration of an IFM receiver:  
(a) IFM receiver, (b) Quadrature detector.

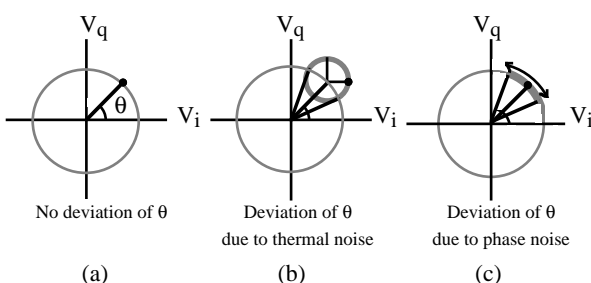


Fig.2. Distribution of output voltages of an IFM receiver :  
(a) Without noise, (b) With thermal noise, (c) With phase noise.

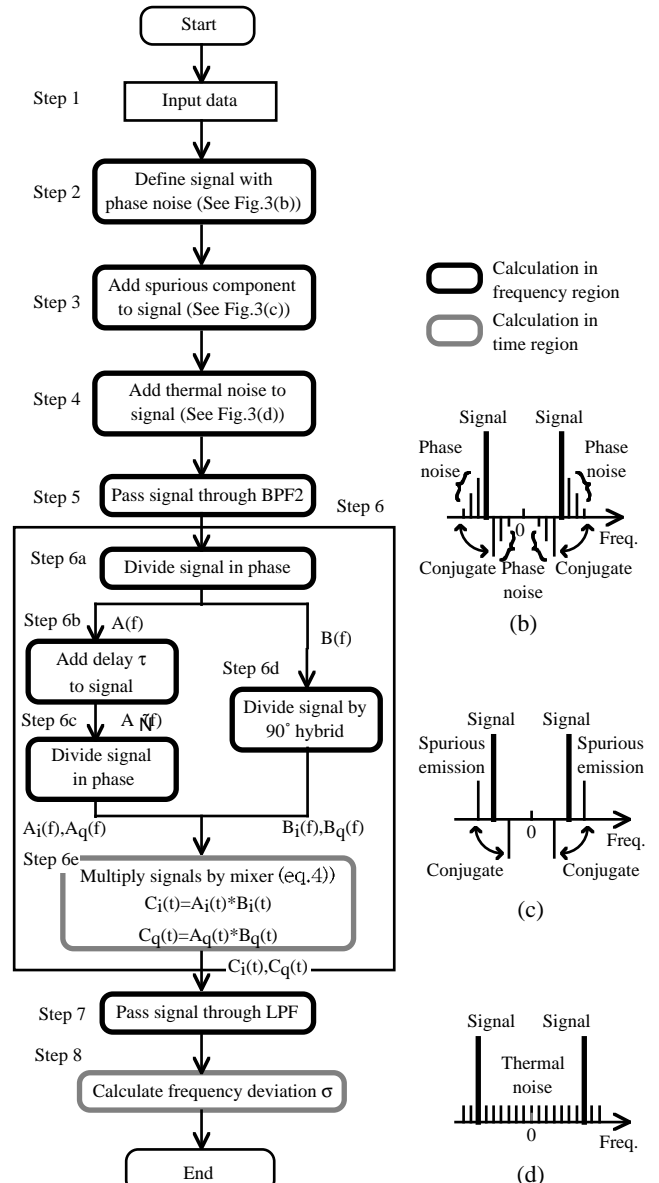


Fig.3. Flow chart of the simulation program: (a) Flow chart, (b) Definition of phase noise, (c) Definition of spurious emissions, (d) Definition of thermal noise.

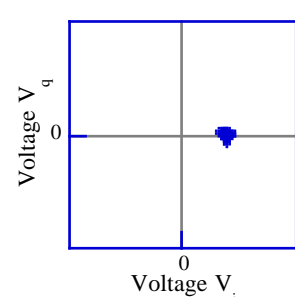


Fig.4. Calculated results of a distribution of output voltages of the IFM receiver with addition of thermal noise  $C/N=25$  dB.

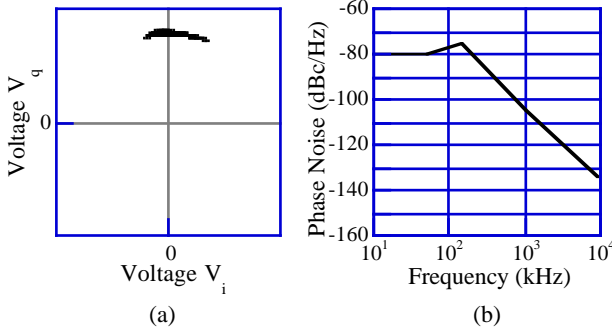


Fig.5. Calculated results of a distribution of output voltages of an IFM receiver when phase noise as shown in Fig. 5(b) is added:  
(a) Calculated results, (b) Added phase noise.

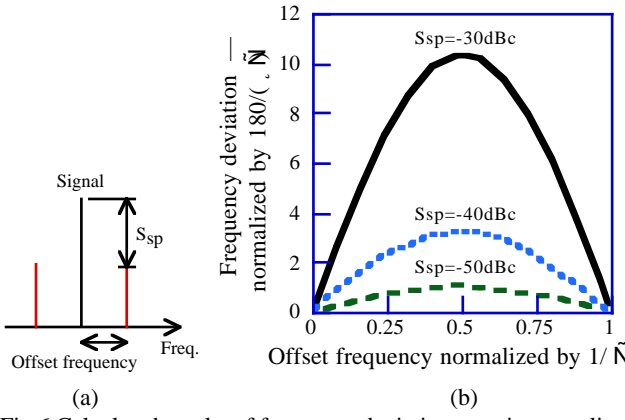


Fig.6. Calculated results of frequency deviation  $\sigma$ .  $\sigma$  is normalized by  $180/(\tau \tilde{N})$ . Offset frequency is normalized by frequency  $1/\tau \tilde{N}$ : (a) Explanation, (b) Calculated results.

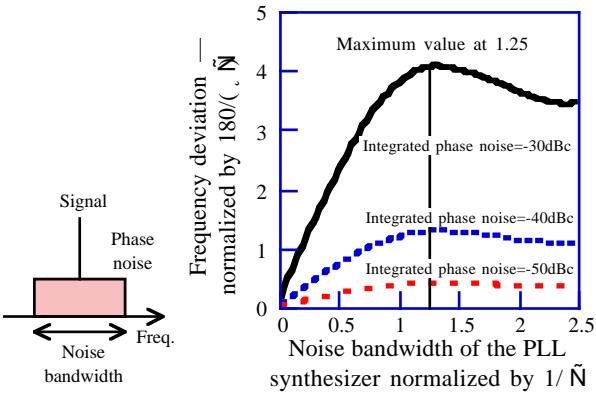


Fig.7. Calculated results of frequency deviation  $\sigma$  with constant integrated phase noise in the noise bandwidth.  $\sigma$  is normalized by  $180/(\tau \tilde{N})$ . The noise bandwidth is normalized by frequency  $1/\tau \tilde{N}$ : (a) Model for phase noise, (b) Calculated results

Table 1 Parameter summary for measurement and calculation

Parameter	Value
Input power of the signal	0 dBm
Offset frequency of spurious emissions	625 kHz
Level of spurious emissions $S_{sp}$	-46 dBc
Thermal noise power	0 to -50 dBm
Phase noise of LO	-80 dBc/Hz@10 kHz -75 dBc/Hz@100 kHz -105 dBc/Hz@1 MHz
Delay of the delay line $t$	800 ns
Order and type of IF BPF	9th order Butterworth
Order and type of LPF	3rd order Butterworth

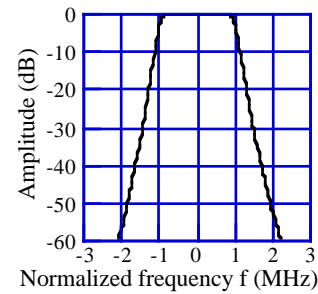


Fig.8. Frequency response of a BPF2.

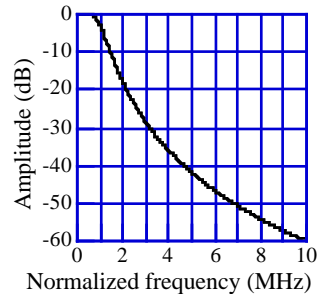


Fig.9. Frequency response of an LPF (LPF<sub>i</sub> and LPF<sub>q</sub>).

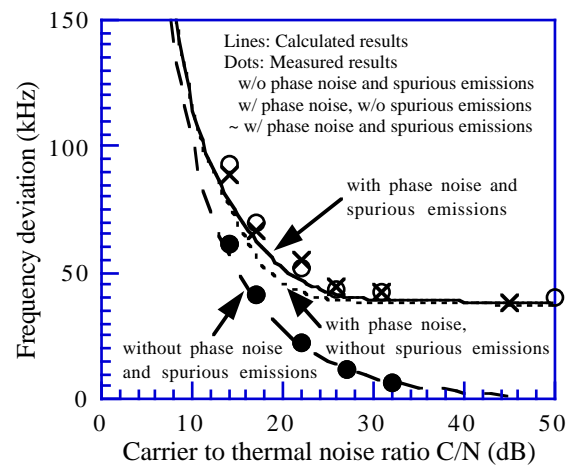


Fig.10. Measured and calculated results of frequency deviation  $\sigma$  with  $\tau=800$  ns. In the figure, lines are calculated results and dots are measured results. Spurious emission is not a major factor to degrade accuracy of measured frequency compared with phase noise of the PLL synthesizer.